Video Article

Surface Potential Measurement of Bacteria Using Kelvin Probe Force Microscopy

Eric Birkenhauer[1], Suresh Neethirajan[1]

[1]BioNano Laboratory, School of Engineering, University of Guelph

Correspondence to: Suresh Neethirajan at sneethir@uoguelph.ca

URL: http://www.jove.com/video/52327
DOI: doi:10.3791/52327

Keywords: Bioengineering, Issue 93, Kelvin probe force microscopy, atomic force microscopy, surface potential, stainless steel, microbial attachment, bacterial biofilms, methicillin-resistant *Staphylococcus aureus*

Date Published: 11/28/2014

Citation: Birkenhauer, E., Neethirajan, S. Surface Potential Measurement of Bacteria Using Kelvin Probe Force Microscopy. *J. Vis. Exp.* (93), e52327, doi:10.3791/52327 (2014).

Abstract

Surface potential is a commonly overlooked physical characteristic that plays a dominant role in the adhesion of microorganisms to substrate surfaces. Kelvin probe force microscopy (KPFM) is a module of atomic force microscopy (AFM) that measures the contact potential difference between surfaces at the nano-scale. The combination of KPFM with AFM allows for the simultaneous generation of surface potential and topographical maps of biological samples such as bacterial cells. Here, we employ KPFM to examine the effects of surface potential on microbial adhesion to medically relevant surfaces such as stainless steel and gold. Surface potential maps revealed differences in surface potential for microbial membranes on different material substrates. A step-height graph was generated to show the difference in surface potential at a boundary area between the substrate surface and microorganisms. Changes in cellular membrane surface potential have been linked with changes in cellular metabolism and motility. Therefore, KPFM represents a powerful tool that can be utilized to examine the changes of microbial membrane surface potential upon adhesion to various substrate surfaces. In this study, we demonstrate the procedure to characterize the surface potential of individual methicillin-resistant *Staphylococcus aureus* USA100 cells on stainless steel and gold using KPFM.

Video Link

The video component of this article can be found at http://www.jove.com/video/52327/

Introduction

Biofilms produced on equipment surfaces and in cutaneous wounds present a problem for the medical industry as biofilms are recalcitrant to removal and can lead to increased rates of disease transmission and antimicrobial resistance. Attachment is the first step in biofilm formation and is the most critical step due to its reversibility[1-3]. Substrate surface characteristics play a crucial role on microbial attachment. Factors such as surface hardness, porosity, roughness, and hydrophobicity have been shown to effect microbial attachment; however, little research examining the role of substrate surface potential (SP) on microbial adhesion has been done[4,5]. Negatively charged surfaces prevent the attachment of *Bacillus thuringiensis* spores to mica, silicon, and gold[6]. Changes in cellular membrane potential are indicative of changes in cellular attachment and motility[5,7]. It has been observed that electrically homogeneous surfaces more readily promote microbial adhesion[5]. Characterizing the surface potential of bacteria at the nanoscale can provide a novel way to understand the adhesion kinetics of bacteria to various surfaces, and thereby can aid in the development of anti-biofouling strategies. Unlike other methods used for characterizing the electro kinetics of bacteria, such as electrophoretic light scattering, zeta potential, and isoelectric point determination, Kelvin probe force microscopy (KPFM) allows for the examination of individual cells instead of entire cultures[8-11]. This is beneficial when wanting to compare cell-cell or biofilm electrical characteristics with high accuracy and precision.

KPFM is a module of atomic force microscopy (AFM). AFM was developed as a direct result of the scanning tunneling microscope (STM)[12]. The first published images using STM were done by Gerd Binnig and Heinrich Rorhrer in 1982[12]. Their invention was able to resolve atomic structures by raster scanning a sharp conductive tip over a conductive surface in air. The implications of achieving high-resolution images excited biologists who quickly attempted to use STM to image dried samples of DNA, proteins, and viruses[12]. STM can also be done in liquids using specialized probe tips[13]. This was shown by Lindsay *et al.*, who used STM and AFM to image DNA molecules in 10 mM $HClO_4$ and in water, on gold electrodes[13]. KPFM has been demonstrated in determining the Surface potentials of DNA and protein analysis[25] and biomolecules interaction with ligands[26].

KPFM operates by measuring the contact potential difference (CPD) between an AFM conductive cantilever tip and an ideally conductive sample (**Figure 1, i**)[14,15]. Samples do not necessarily have to be conductive (*i.e.,* biological samples). Imaging can be carried out on mica, glass, and silicon surfaces (non-conductive) as long as the non-conductive surface is thin and there is an underlying conductive material[6,7]. The CPD is equivalent to the surface potential voltage and can be described as the difference in the work functions between the tip (φ_{tip}) and sample (φ_{sample}), divided by the negative electron charge (-*e*). When a conductive AFM tip is brought close to a sample surface (separated by distance *d*), an electrostatic force (F_{es}) is generated due to the difference in Fermi energies (**Figure 1, ii, a**)[15]. At this point, the vacuum energies of the tip and sample (E_v) are in equilibrium and aligned. Upon bringing the tip closer to the sample surface, the tip and sample surface come

into electrical contact and act as parallel plate capacitors (**Figure 1, ii, b**)[14,15]. At the point, the Fermi energies of the tip and sample surface become aligned, reaching a steady-state equilibrium (**Figure 1, ii, b**). The tip and sample surface will be charged and a V_{CPD} will form due to a difference in E_V's and work functions. A F_{es} acts on the electrical contact area due to the formed V_{CPD}. This force is subsequently nullified through the application of an external V_{DC} to the tip that has the same magnitude as the formed V_{CPD} (**Figure 1, ii, c**). This applied DC voltage eliminates surface charge in the area of electrical contact, and the amount of V_{DC} necessary to eliminate the F_{es} of V_{CPD} is equal to the difference in the work functions between the sample surface and tip[15]. It should be noted that the work function of the tip is known and it is provided by manufacturers. In all KPFM methods, an AC voltage (V_{AC}, approximately 100 - 500 mV) is also applied to the tip in order to generate oscillating electrical forces between the tip and sample[14]. This provides better resolution when measuring changes in V_{CPD} and/or F_{es}. In this regard, changes in the frequency or amplitude of electrical oscillation can be corrected by V_{DC}, and surface potential maps can be generated. Data from specific areas of these maps can be further analyzed to provide electrical information about specific topographical features.

KPFM can be operated in three modes: (1) lift mode, (2) amplitude modulation (AM) mode, and (3) frequency modulation (FM) mode[14,16]. Lift mode was the initial incarnation of KPFM. Lift mode relies on a two-pass method in which an oscillated tip is dragged across the surface to obtain a topographical image. For the second pass the tip is raised a preset distance above the sample (10 - 100 nm) and scanned back across the same area. Due to this two-pass method, lift mode, compared to AM- and FM-KPFM, takes the longest time for image acquisition. Raising the tip away from the surface ensures that only long-range F_{es} is measured. Also, cross talk between topography and surface potential measurements is decoupled at the expense of increased lateral resolution and sensitivity.

AM-KPFM improves lateral resolution and sensitivity by using dual-frequencies to simultaneously measure sample topography and surface potential (one-pass scan)[14]. In AM mode, the cantilever is mechanically oscillated, generally 5% below its first resonant frequency (f_0), and electrically oscillated (through a V_{AC}) at its second resonant frequency (f_1). Changes in the amplitude of f_0 lead to the generation of topographical data, while changes in the amplitude of f_1, due to changes in F_{es} and V_{CPD}, give surface potential measurement data. f_0 and f_1 of the cantilever are separated by significant frequencies and energies that signal cross-talk is minimized[14]. The head electronics box (HEB) of the AFM separates out the two signals to give both topographical and surface potential data simultaneously in one scan. FM-KPFM improves resolution even further than AM-KPFM on biological surfaces[14]. FM-KPFM works differently than AM-KPFM in that it measures changes in electrostatic force gradients rather than electrostatic force (F_{es})[15]. Like AM mode, FM mode utilizes dual-frequencies and a single-pass scanning mechanism to obtain topographical and surface potential data simultaneously[14]. In FM mode, the cantilever is mechanically oscillated at f_0 and electrically oscillated at a low modified frequency (f_{mod}, typically 1 - 5 kHz). Upon electrostatic interactions, f_0 and f_{mod} mix to produce side bands $f_0 \pm f_{mod}$. These sidebands are very sensitive to changes in electrostatic force, and can be separated from f_0 through the AFM's HEB. Since FM-KPFM measures changes in electrostatic force gradients, the tips apex shape and its maintenance/integrity play a critical role in overall surface potential resolution[14, 15]. Surface potential resolution using AM and FM modes are in the range of 1 nm laterally[14-16]. It should be noted that KPFM imaging can be done in non-polar liquids, and more recently, has been shown to be done in low-ionic (<10 mM) polar liquids (in open-loop KPFM modes which do not require a bias feedback, obviating the application of a DC bias) such as MilliQ water; however, KPFM imaging has yet to be done on live cells in polar solutions[17-20]. Additional challenges associated with SP imaging in liquid is that solutions commonly used for maintaining cells (*i.e.,* phosphate buffered saline) have high concentrations of mobile ions, which would lead to Faradaic reactions, bias-induced charge dynamics, and ion diffusion/redistribution[20]. Thus, for this experiment, measurements were taken from dried and dead MRSA cells on poly-L-lysine functionalized stainless steel and gold surfaces under ambient conditions. Imaging can be carried out in air or vacuum conditions on biological samples that have been previously dried or immobilized onto surfaces[20]. Humid conditions have also been shown to affect KPFM imaging of surfaces[6].

In this study, we employed FM-KPFM and AFM to examine the role of SP on the attachment of methicillin-resistant *Staphylococcus aureus* USA100 (MRSA) to poly-L-lysine functionalized stainless steel and gold surfaces. MRSA has recently garnered status as a multi-drug resistant (MDR) "superbug" due to its naturally selected resistance to many β-lactam antibiotics and cephalosporins[21]. MRSA infections are now more challenging, difficult, and formidable to treat, leading to the use of harsher antimicrobials such as vancomycin or oxazolidinones which have higher toxicity levels in humans, and therefore cannot be used as long-term treatments[22]. Stainless steel was chosen due to its medical relevance and common use as a material in hypodermic needles, bedpans, door handles, sinks, etc. Gold was used as a comparative metal. FM-KPFM was utilized to examine if microbial membrane SP changes upon attachment to the substrates.

Protocol

1. Preparation of Glassware and Cultures

1. Before proceeding with this experiment, prepare 5% sheep's blood agar (SBA) plates for growing MRSA. Incubate SBA plates for 24 hr at 37 °C. After this time, single, well-isolated colonies should be present to be used for subsequent inoculations into liquid media. Store streaked SBA plates with single colonies at 4 °C for 1 - 2 months.
   NOTE: Sheep's blood agar plates come in pre-made packs containing between 20 - 25 plates based on the manufacturer, and typically consist of a tryptic soy agar base with the addition of 5% w/v sheep's blood.
2. Make 500 ml of tryptic soy broth (TSB) supplemented with 1% glucose and 0.1% NaCl. After this, collect and clean 2 glass test tubes. If autoclavable lids are unavailable for test tubes, use aluminum foil as a cap. Autoclave TSB and test tubes along with a box of 1 ml pipette tips.
3. Under a biosafety cabinet or near a Bunsen burner, pipette 5 ml of previously autoclaved TSB into autoclaved test tubes. Be careful to ensure that enough time has been given to let the TSB and test tubes cool to room temperature. From a previously streaked 5% SBA plate, inoculate a single colony into 6 ml TSB broth. One will contain MRSA, and the second test tube will be used as a negative control to ensure sterility.
4. Take inoculated TSB test tubes and place them in a reciprocal incubator for 24 hr at 37 °C and at 200 rpm. After this time microbial growth should be apparent in the MRSA test tube while no growth should have occurred in the control test tube.
5. Take 1 ml from 24 hr culture and pipette into 6 ml of fresh TSB. Incubate at 37 °C for 6 hr at 200 rpm.
6. Pipette 1 ml of 6 hr sub-culture into a 1.5 ml microfuge tube. Centrifuge for 3 min at 850 x g. Remove supernatant and re-suspend pellet in 1 ml of deionized H_2O. Centrifuge, repeat, and re-suspend.

2. Cleaning and Inoculation of Stainless Steel and Gold Substrates

1. Take stainless steel and gold AFM sample disks (20 mm and 10 mm diameters respectively) and clean each side with 5 ml of deionized H_2O. Hold sample disks in the dominant hand with forceps and use the subdominant hand to pipette 5 ml on each side of the sample disk. After washing both sides, place sample disks in a beaker containing 20 ml of deionized H_2O followed by sonication for 1 min.
2. After sonication use forceps to remove sample disks from the beaker. Place the disks so that they lean at a 60° angle against the edge of an open Petri plate onto a paper towel. Use the lid of the Petri plate to cover the drying disks. Let disks dry fully before proceeding. The drying time can vary between 4 - 8 hr.
3. Once dry, use forceps to place sample disks into a Petri plate.
    1. Optionally, functionalize the surfaces of sample disks with any material (*e.g.,* collagen, hyaluronan, silver nano-particles, *etc.*).
    2. For this experiment, use poly-L-lysine to coat the substrate surface. For poly-L-lysine functionalization, pipette 200 - 400 µl of 0.1% poly-L-lysine (in H_2O) onto sample disks, and let incubate for 1 hr at room temperature in a Petri dish.
    3. After 1 hr, use forceps to hold the sample disk, and wash with 1 ml of deionized H_2O. Let dry on paper towels as described in **step 2.2**.
4. Take 2x washed re-suspended cells and plate 200 - 400 µl onto sample disks inside a biosafety cabinet. If sample disks are coated with poly-L-lysine, incubate for 0.5 hr at room temperature.
5. After incubation of cells on sample disks, wash sample disks gently with 1 ml of deionized H_2O. Let disks dry overnight before imaging.

3. KPFM Imaging

NOTE: For this experiment, use an Agilent 5500 series ILM-AFM.

1. To start AFM, turn on computer unit along with the AFM's HEB and MAC III controller. Open AFM imaging software (*e.g.,* Agilent's PicoView). Be sure to initially select ACAFM or whichever the correct designation is on the AFM for imaging in intermittent-contact mode.
2. Using AFM forceps in the dominant hand, and holding the spring-loaded clip holder open with the subdominant hand, place a KPFM cantilever into to head-piece. Be careful when handling and transferring the AFM head-piece to the AFM as this unit (at least on the 5500 ILM-AFM) contains the fragile piezo crystal unit that controls X, Y, and Z scanning directionalities.
   NOTE: The KPFM cantilevers used in this case were Mikromasch conductive DPE (low-noise) cantilevers with average resonant frequencies of 80 kHz and spring constants of 2.7 N/m. Cantilevers with these resonant frequencies and spring constants were chosen due to their ease of use. Cantilevers with larger spring constants and higher resonant frequencies can also be used for imaging.
3. Carefully load head-piece into the AFM and connect the appropriate wires (in this case two wires need to be plugged in: laser light and stage lift motor).
4. Align the laser onto the tip of the cantilever. Some units contain a camera functionality which allows for easier alignment. If camera functionality is not present on AFM, align onto the cantilever tip as described next:
    1. Rotate the front-to-back knob clockwise to move the laser overtop the cantilever chip. When the laser reaches the chip it will be blocked and will no longer be visible. Only turn the knob a few times.
    2. Rotate the front-to-back knob counterclockwise until the laser spot reappears. The laser is now on the chip's edge.
    3. Rotate the left-to-right knob to position the laser on the cantilever. As the laser passes over the cantilever it will disappear and reappear in rapid succession. The laser spot should be visible in the frosted glass cover where the photodiode unit will later sit.
    4. Turn the front-to-back knob counterclockwise to move the spot down the cantilever towards the tip until the spot on the frosted glass disappears.
    5. Turn the front-to-back knob clockwise only slightly in order to position the laser so that it just sits on the cantilever tip. The laser spot will reappear on the frosted glass.
       NOTE: This is the laser positioning method for diving-board cantilevers. For triangular cantilevers, the alignment process differs slightly.
5. Once the laser is aligned, hold the stage lift motor in the "open" position for 10 sec to ensure enough space between the cantilever and sample when attaching the sample to the AFM.
6. Place sample on the KPFM sample stage. Ground the sample using a copper wire. Connect the appropriate wires from the AFM to the sample stage. Connect the stage to the AFM. In most cases the stage is held in place using magnets.
7. In the AFM software, tune the cantilever and then begin approach of the cantilever tip to the sample. Ensure that settling time is set at no more than 10 msec, and that approach speeds do not exceed 2.0 µm/sec in order to avoid tip damage.
8. Once the cantilever tip is on the sample surface, select an imaging window size and ideal imaging area. Optimize I and P gains along with the cantilever set point so that topographical imaging is optimized.
    1. Once topographical imaging is optimized, turn on KPFM module (either FM or AM mode; here, use FM mode). It should be noted that KPFM imaging is very challenging outside of 5 µm x 5 µm imaging window. Also, for optimal KPFM imaging, use a 512 x 512 resolution with slow scan speeds (0.02 - 0.05 lines/sec).
9. For FM-KPFM settings (not ACAFM settings), set the drive percent between 5 - 10%. Set the cantilever frequency between 1 - 5 kHz with a bandwidth of 2 kHz. Set I and P gains for the FM-KPFM settings to 0.3%.
    1. Vary signal bandwidth and I and P gains between sample surfaces. To optimize SP imaging, further adjust signal bandwidth and I and P gains to obtain optimal images. The recommended range of I and P gains are from 0.22 - 0.35%.
10. Process and analyze collected KPFM images using post-image processing software to collect SP data.

Representative Results

The ability to measure SP using KPFM relies on the principle that both the sample surface and cantilever tip are conductive to some extent. Stainless steel and gold acted as conductive surfaces to which MRSA were attached. KPFM images were taken of 15 MRSA cells on both

surfaces with 512 x 512 resolutions, and with scan areas ranging from 5 x 5 µm to 10 x 10 µm. Scanning was carried out with line speeds ranging from 0.02 lines/sec to 0.05 lines/sec. Therefore, with 512 data points collected per line and 512 lines to scan, scan times ranged from 2.84 hr to 7.11 hr. The types of images collected can be seen in **Figure 2**. KPFM operates using dual frequencies, and as such, topographic images are simultaneously collected along with data about the electrical characteristics of the surface. Thermal filters were applied to SP maps in order to more easily discern small changes in surface potential (**Figure 2**). Data from SP maps was analyzed post-image processing software to determine average surface potentials and standard deviations. Statistical analysis was performed using R Open Source Statistical Programming. Student t-tests were performed to compare groups with $P < 0.05$ being considered significant.

SP images were analyzed to determine microbial membrane surface potential. These were then compared with the growth on the different substrate surfaces. This was done in order to determine if surface type had an effect on microbial membrane surface potential. Initially we attempted to incubate MRSA cells statically for 3 hr on the substrate surfaces. However, no attached microbes were visible under the AFM. SP data for clean and poly-L-lysine functionalized surfaces was determined from 5 x 5 µm scanned areas. SP scans of the bare stainless steel and bare gold substrates showed overall negative surface potentials (-0.045 ± 0.057 V and -0.126 ± 0.052 V, respectively, $P = 0.047$, **Figure 3**). Poly-L-lysine was used in order to functionalize the surfaces to make them more favorable for cell attachment. Functionalized surfaces showed a shift to positive surface potentials for stainless steel and gold surfaces (0.133 ± 0.063 V and 0.126 ± 0.030 V, respectively, **Figure 3**). We subsequently examined the membrane potentials of MRSA on poly-L-lysine functionalized stainless steel and gold surfaces. It was found that MRSA cell membrane potentials varied between stainless steel and gold surfaces. Stainless steel surfaces led to significantly larger positive membrane SPs for cells when compared to their gold counterpart. For example, the SP of MRSA cells switched from positive to negative SPs. MRSA showed positive SP on stainless steel surfaces with SPs of 0.160 ± 0.022 V and SP of -0.025 ± 0.016 V on gold surfaces ($P < 0.001$).

To show the full capabilities of KPFM, an example of a step-height graph of MRSA on stainless steel is provided (**Figure 4**). This shows the difference in surface potential between the substrate surface and the microbial membrane.

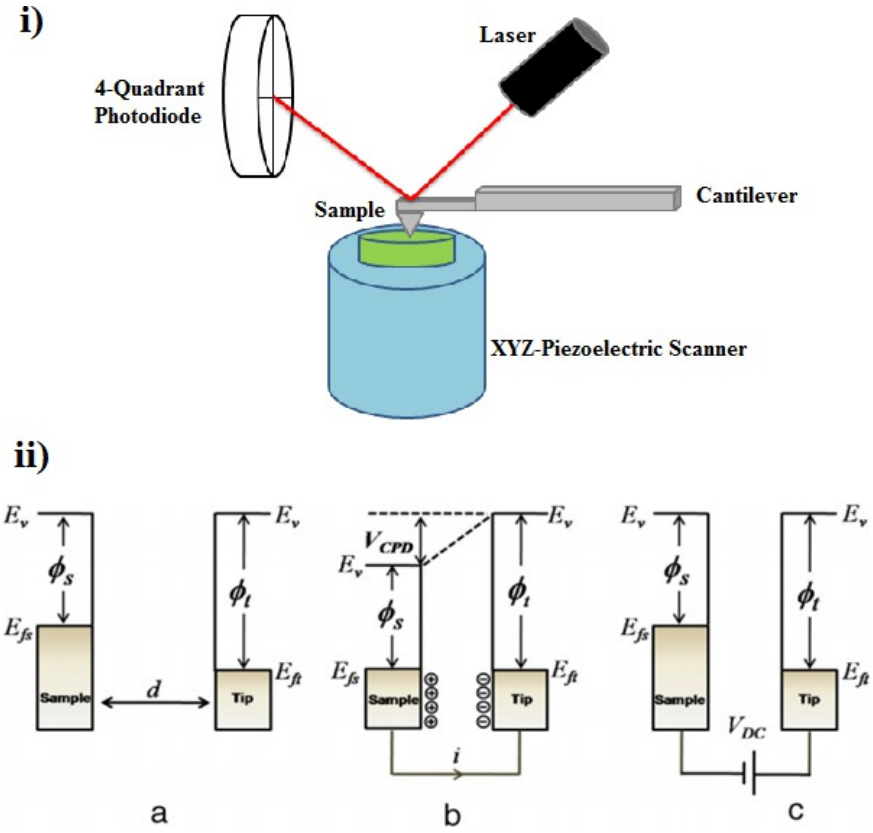

Figure 1. Working principles of atomic force microscope (i) and Kelvin probe force microscope (ii) Reprinted with permission from (15). The basic configuration of AFM is shown in (i). In AFM, a sharpened tip is attached to a cantilever through electrochemical deposition. Mikromasch platinum-coated conductive DPE (low-noise) cantilevers were used in this experiment had dimensions of 210 x 30 µm, 80 kHz resonance frequency, and spring constants of 2.7 N/m. Cantilevers were attached to a larger chip in order to allow for easy handling. Once assembled in the AFM, a laser is aligned onto the cantilever tip. Deflections in the cantilever tip are detected through a photodiode. Deflections are used to generate topographical images. (ii, a, b, c) shows the working principle of KPFM. The cantilever is brought close enough to the surface to allow for electrical contact to occur. Differences in the surface potentials between the tip and surface cause the tip to deflect. A DC voltage is applied to correct for this deflection. This DC applied voltage is equal to the surface potential of the substrate surface. Depending on the type of imaging mode used (lift, AM, FM), this working principle differs slightly. Figure 1(ii) has been modified from[15].

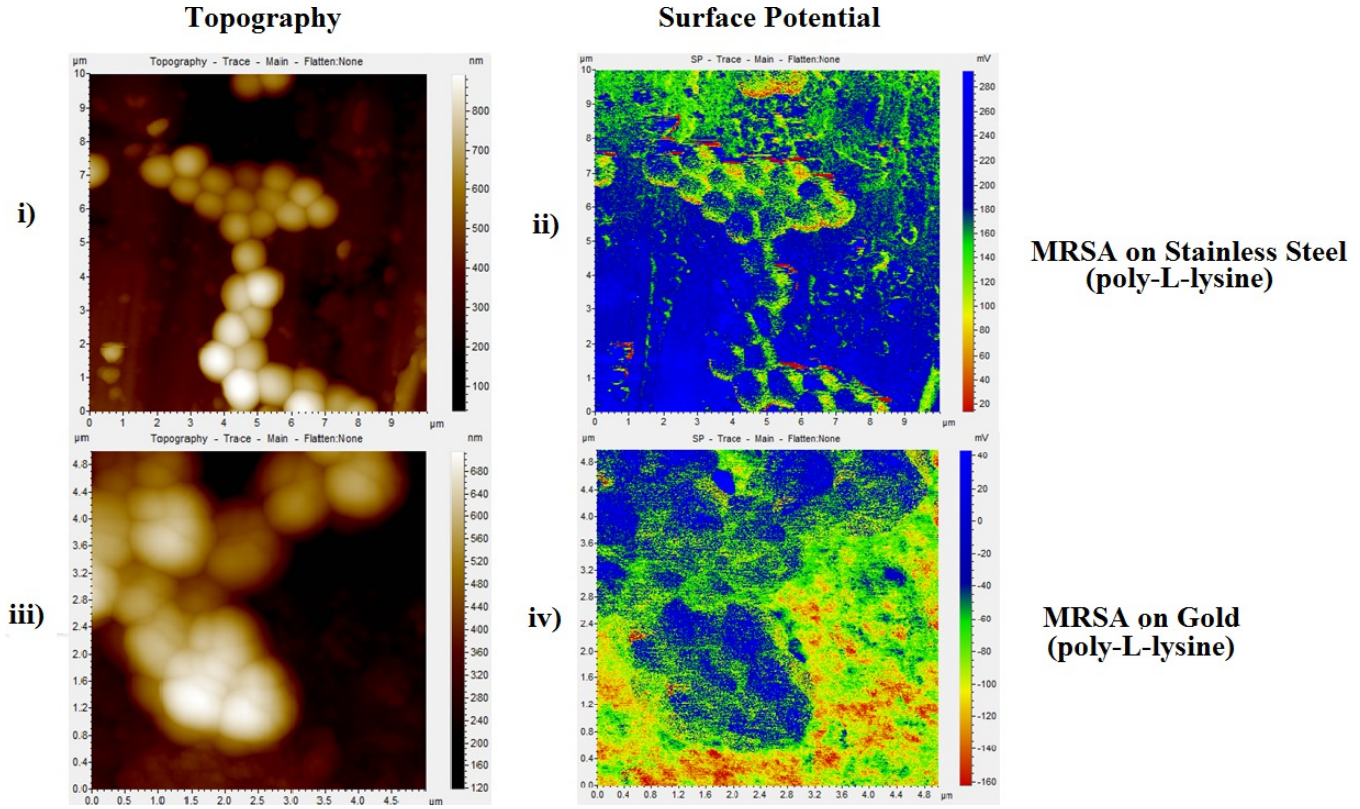

Figure 2. Representative topography and surface potential maps of MRSA on poly-L-lysine functionalized stainless steel and gold substrates. Images (i and iii) show representative topography images of MRSA cells on stainless steel and gold surfaces, respectively. Image dimensions can be seen in the X and Y axis of these images along with a corresponding colored height profile. (ii and iv) show the corresponding SP maps of the MRSA on their respective surfaces. Standard 'gold' color filters were applied to topography images while thermal filters were applied to SP images to more easily discern small changes in SP. It should be noted that the SP of substrate surfaces was not homogenous. SP was found to be heterogeneously distributed with apparent positive and negative areas on both substrate surfaces. This can be seen around MRSA cells where heterogeneous SPs are observed on stainless steel and gold substrates. Please click here to view a larger version of this figure.

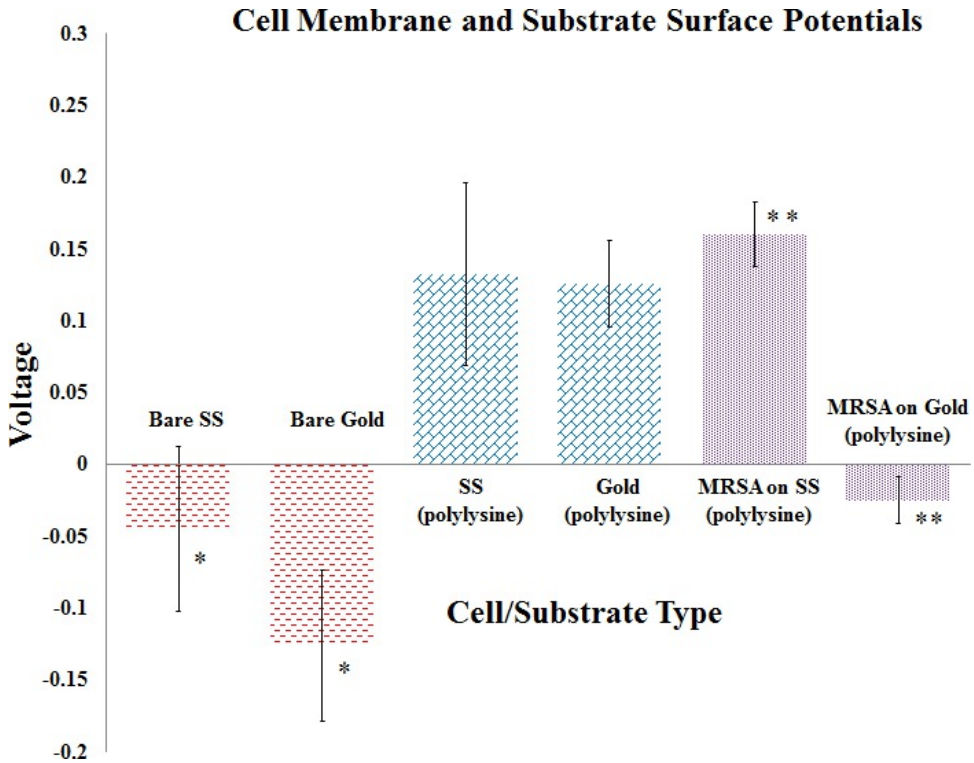

Figure 3. Surface potential of substrate surfaces and MRSA cellular membranes. **Figure 3** shows the corresponding KPFM data from stainless steel (labeled here as SS) and gold surfaces, as well as, data from 15 cells. Asterisks represent significant differences between samples with the number of asterisks corresponding to the compared samples. MRSA data was collected from cells attached to functionalized surfaces after 30 min of incubation. This was done due to the fact that no cells were found to attach to the bare substrate surfaces after 3 hr.

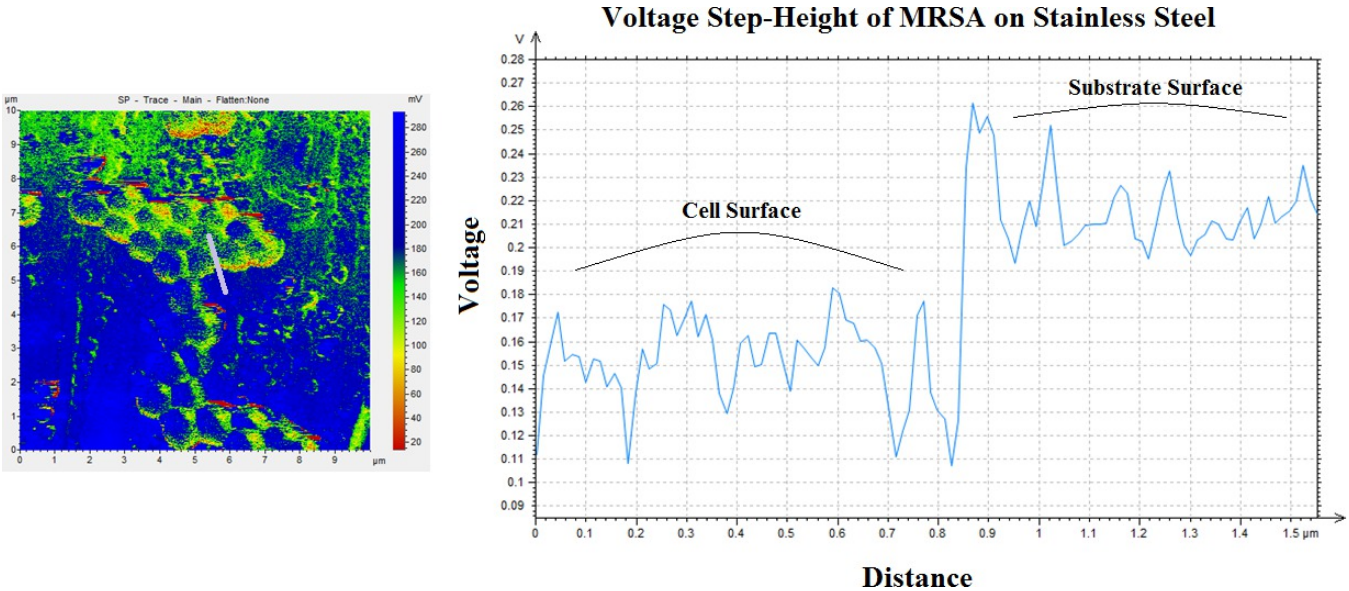

Figure 4. Step-height surface potential image of MRSA on poly-L-lysine functionalized stainless steel. Using post-image processing software, a step-height graph was generated in order to show the capabilities of the software, as well as, the noticeable difference in SP between the substrate surface and cell membrane. The cross-sectional area chosen is represented on the corresponding SP map with the grey line. A shift from 0.15 V on the cell surface to 0.21 V on the substrate surface is clearly apparent. Please click here to view a larger version of this figure.

Company	Probe Type	Spring Constant (N/m)	Resonant Frequency (kHz)	Cantilever Dimensions	Tip Apex Diameter
Asylum Research	AC240TM-R3	2	70	Length = 240 µm Width = 40 µm	28 nm
Bruker AFM Probes	SCM-PIT	2.8	75	Length = 225 µm Width = 28 µm	20 nm
Mikromasch	Conductive DPE (Low-Noise) Cantilevers	2.7	80	Length = 210 µm Width = 30 µm	40 nm
Nano and More USA	PtSi-NCH	42	330	Length = 125 µm Width = 30 µm	>25 nm
Nanoscience Instruments	AppNano Conductive Tapping Mode AFM Probes.	40	300	Length = 125 µm Width = 35 µm	30 nm
Nanoscience Instruments	AppNano Conductive Tapping Mode AFM Probes.	40	300	Length = 125 µm Width = 35 µm	30 nm

Table 1. Companies offering a wide range of KPFM probes. A variety of companies now offer KPFM tip with varying tip apex diameters, spring constants, and resonant frequencies. Tip customization is near limitless, with companies typically offering to build cantilevers with custom specifications for an intended experiment. Most KPFM probes are platinum coated silicon nitride. Platinum provides conductive functionality to the cantilever. Other common coating materials include iridium, platinum + iridium, and gold. Most KPFM tips can also be alternatively used for electric force microscopy (EFM). Tip apex is important for KPFM cantilevers. Larger diameter tips sacrifice higher resolution topography imaging for less electrical noise. Conversely, smaller diameter tips (<25 nm) offer improved topography image resolution but are more prone to electrical noise. For this study, researchers used Mikromasch conductive DPE (low-noise) cantilevers.

Discussion

KPFM was employed as a novel technique for obtaining surface electrical data. It has commonly been used as a method for examining charge distribution in chemistry and has only recently begun to be applied for the study of biological systems on the micro- and nano-scales. From the data collected we found that microbes did not appear to readily attach to clean stainless steel and gold surfaces, even after 3 hr of static incubation. Poly-L-lysine functionalized surfaces showed rapid microbial attachment after 30 min. Longer incubation times of microbes on functionalized surfaces led to cell overcrowding on sample surfaces, and poor topography images. Surface functionalization led to a shift from negative SP to positive SP for stainless steel and gold surfaces. Previous studies have shown that microorganisms typically have negative SPs due to the sequestering of negatively charged ions around cells to maintain osmotic and ionic balance[23]. It is also known that the presence of phosphate groups in Gram negative microorganisms and teichoic acids in Gram positive microorganisms further leads to the formation of negative SPs[24]. Knowledge of the basic chemistry of Gram positive and negative cell membranes led us to assume that positive substrate SPs would lead to rapid microbial attachment. However, as can be seen in **Figures 2 - 4**, that there was a large shift from positive to negative MRSA cell SPs on stainless steel and gold substrates, respectively. Microbial attachment could have initially occurred from the sequestration of negative ions around the membrane. Upon washing the cells and letting them dry on the substrate surfaces, we could have been washing away this ionic media. Also, it should be noted that KPFM data is only inclusive of the outer cell wall areas of the Gram positive (MRSA) cells. It has been shown in some cases that a microorganisms cell membrane potential may change upon the presence of cationic antimicrobial peptides or other stressors[8].

The one main disadvantage of KPFM compared to standard zeta potential measurements on microbial cell cultures is that in KPFM the data collected is done on dead and dried cells. KPFM was used to examine general trends in cell surface potential shifts with regards to different attachment substrate surfaces. The application of DC voltages to the cantilever tip (to counteract F_{es}), along with the requirement of a conductive sample surface, limit standard KPFM to open-air imaging. Imaging in polar liquid is not currently possible with standard KPFM, and thus the imaging of live cells using KPFM is not as of yet possible. Developments of new open-loop and dual frequency KPFM modes have shown promise in their ability to image surfaces in low-ionic solutions[18-20]. It is our hope that in the future this technology is further developed so that imaging can be done on live cell cultures. The imaging of cells in a more natural environment would undoubtedly lead to the generation of more accurate and realistic cell membrane SP data. For this study we wanted to apply this technology in a novel way to measure microbial cell membrane potentials, as well as study the adhesion characteristics of MRSA on a medically relevant surface. Changes in microbial membrane SPs were observed upon incubation on the different substrate surfaces. This may imply that substrate type may affect cellular metabolism. Our hope is that this preliminary data may lead to the generation of nano-coatings with inherent electrical charges that could be applied to medical surfaces or equipment (including other materials such as bandages and gauzes) in order to prevent microbial attachment. The protocol described within this article is intended to help researchers understand the principles of KPFM and show ways in which it can be applied to measure and create SP maps.

Disclosures

The authors have nothing to disclose.

Acknowledgements

The authors sincerely thank the Natural Sciences and Engineering Research Council of Canada, the Ontario Ministry of Research and Innovation, and the Canada Foundation for Innovation for funding this study.

References

1. Seth, A.K., *et al*. *In vivo* modeling of biofilm-infected wounds: a review. *J. Surg. Research.* **178** (1), 330-338 (2012).
2. Wolcott, R.D., & Ehrlich, G.D. Biofilms and chronic infections. *JAMA*. **299** (22), 2682-2684 (2008).
3. Hoiby, N., *et al*. The clinical impact of bacterial biofilms. *Micro. Infect*. **3** (2), 55-65 (2011).
4. Zhang, W., Hughes, J., & Chen, Y. Impacts of hematite nanoparticle exposure on biomechanical, adhesive, and surface electrical properties of *E. coli* cells. *Appl. Environ. Microbiol.* **78** (11), 3905-3915 (2012).
5. Lorite, G.S., *et al*. Surface physicochemical properties at the micro and nano length scales: role on bacterial adhesion and *Xylella fastidiosa* biofilm development. *PLoS One*. **8** (9), doi: 10.1371/journal.pone.0075247 (2013).
6. Lee, I., Chung, E., Kweon, H., Yiacoumi, S., & Tsouris, C. Scanning surface potential microscopy of spore adhesion on surfaces. *Coll. Surf. Biointer.* **92**, 271-276 (2012).
7. Tsai, C., Hung, H., Liu, C., Chen, Y., & Pan, C. Changes in plasma membrane surface potential of PC12 cells as measured by Kelvin probe force microscopy. *PLoS One*. **7** (4), DOI: 10.1371/journal.pone.0033849 (2012).
8. Jucker, B.A., Harms, H., & Zehnder, A.J. Adhesion of the positively charged bacterium *Strenotrophomonas* (*Xanthomonas*) *maltophilia* 70401 to glass and Teflon. *J. Bacteriology*. **178** (18), 5472-5479 (1996).
9. Soon, R.L., *et al*. Different surface charge of colistin-susceptible and -resistant *Acinetobacter baumannii* cells measured with zeta potential as a function of growth phase and colistin treatment. *J. Anti. Chemo*. **66**, 126-133 (2011).
10. Tariq, M., Bruijs, C., Kok, J., & Krom, B.P. Link between culture zeta potential homogeneity and Ebp in *Enterococcus faecalis*. *Appl. Environ. Microbiol.* **78** (7), 2282-2288 (2012).
11. Ayala-Torres, C., Hernandez, N., Galeano, A., Novoa-Aponte, L., & Soto, C. Zeta potential as a measure of the surface charge of mycobacterial cells. *Ann Microbiol.* doi: 10.1007/s13213-013-0758-y (2013).
12. Allison, D.P., Mortensen, N.P., Sullivan, C.J., Doktycz, M.J. Atomic force microscopy of biological samples. *Nanomed. Nanobiotech.* **2** (6), 613-634 (2010).
13. Lindsay, S.M., *et al*. Scanning tunneling microscopy and atomic force microscopy studies of biomaterials at a liquid-solid interface. *J. Vac. Sci. Technol.* **11** (4), 808-815 (1993).
14. Moores, B., Hane, F., Eng, L., & Leonenko, Z. Kelvin probe force microscopy in application to biomolecular films: frequency modulation, amplitude modulation, and lift mode. *Ultramicroscopy*. **110** (6), 708-711 (2010).
15. Melitz, W., Shen, J., Kummel, A.C., & Lee, S. Kelvin probe force microscopy and its application. *Surf. Sci. Reports.* **66** (1), 1-27 (2011).
16. Loppacher, C., *et al*. FM demodulated Kelvin probe force microscopy for surface photovoltage tracking. *Nanotechnology*. **16** (3), doi:10.1088/0957-4484/16/3/001 (2005).
17. Domanski, A.L., *et al*. Kelvin probe force microscopy in nonpolar liquids. *Langmuir*. **28** (39), 13892-13899 (2012).
18. Collins, L., *et al*. Dual harmonic Kelvin probe force microscopy at the graphene-liquid interface. *Appl. Phys. Letters.* **104** (13), 133103 (2014).
19. Kobayashi, N., Asakawa, H., Fukuma, T. Nanoscale potential measurements in liquid by frequency modulation atomic force microscopy. *Rev. Sci. Instru.* **81**, 10.1063/1.3514148 (2010).
20. Collins, L., *et al*. Probing charge screening dynamics and electrochemical processes at the solid-liquid interface with electrochemical force microscopy. *Nature Comm.* **5**, 2871, doi: 10.1038/ncomms4871 (2014).
21. Pastar, I., *et al*. Interactions of methicillin resistant *Staphylococcus aureus* USA300 and *Pseudomonas aeruginosa* in polymicrobial wound infection. *PLoS One*. **8** (2), doi:10.1371/journal.pone.0056846 (2013).
22. Brien, D.J., & Gould, I.M. Does vancomycin have a future in the treatment of skin infections? *Cur. Opin. Infec. Diseas.* **27** (2), 146-154 (2014).
23. Wang, P., Kinraide, T.B., Zhou, D., Kopittke, P.M., & Peijnenburg, W.J.G.M. Plasma membrane surface potential: dual effects upon ion uptake and toxicity. *Amer. Soc. Plant. Biol.* **155** (2), 808-820 (2011).
24. Gross, M., Cramton, S.E., Gotz, F., & Peschel, A. Key role of teichoic acid net charge in *Staphylococcus aureus* colonization of artificial surfaces. *Infect. Immun.* **69** (5), 3423-3426 (2001).
25. Sinensky, A.M., & Belcher, A.M. Label-free and high-resolution protein/DNA nanoarray analysis using Kelvin probe force microscopy. *Nat. Nanotechnol.* 2, 653-659 (2007).
26. Park, J., *et al*. Single-molecule recognition of biomolecular interaction via kelvin probe force microscopy. *ACS Nano*. **5** (9), 6981-6990 (2011).

